Branch-Point Motion in Asymmetric Star Polymers

Jung Hun Lee, Lewis J. Fetters, and Lynden A. Archer*

School of Chemical and Biomolecular Engineering, Cornell University, Ithaca, New York 14853

Received November 10, 2004; Revised Manuscript Received March 9, 2005

ABSTRACT: Linear viscoelastic behavior of a series of 1,4-polyisoprene asymmetric star polymers was investigated experimentally and theoretically in order to determine how branch point motion affects terminal relaxation dynamics. For the systems studied, the branch point is connected to a moderately entangled short arm ($M_B/M_e = 7$) and two longer arms with varying numbers of entanglements ($M_A/M_e = 7-43$). The measured loss modulus manifests a clear transition from starlike to linear-like dynamics as the molecular asymmetry increases. We show that this behavior can be predicted using a tube-model for branched molecules (Frischknecht et al. *Macromolecules* **2002**, *35*, 4801) with a self-consistently determined branch-point diffusivity, $D_{bp} = (p a_0)^2/2\tau_{a,B}$. Here a_0 is the effective bare tube diameter, $\tau_{a,B}$ is the arm retraction time, and $p^2 = 1/[(2N_{AR})b^2/a_0^2]$ is an effective drag produced by unrelaxed backbone segments. We also compare relaxation moduli predicted by the tube model with experimental data and find good agreement over a range of short- and long-arm entanglement densities.

1. Introduction

The effect of polymer architecture on liquid state rheological properties is a subject of importance in polymer science due to a prospective impact on industrial polymers. Fundamental studies of stress relaxation dynamics of well-characterized high molecular weight polymers with multiple, long side branches are nonetheless quite rare. The main difficulties come from the fact that there are a lot of structural factors to be considered. The length of branch, the distribution of branches, the branching arrangement, and the resulting backbone (or cross-bar) length between adjacent branch points profoundly affect rheological properties such as zero shear viscosity η_0 and terminal relaxation time τ_0 of slightly different nonlinear structures with similar molecular weight. Several recent studies of polymers with model branched architectures including star,[1,2] H-shaped,[3] multiarm pompom,[4−6] and comb[7] polymers provide promising framework in which the effect of long side branches on polymer relaxation dynamics can be studied. Findings from these studies appear to confirm the basic proposal of McLeish's branched polymer theory, namely that branched polymers relax *hierarchically*.[3]

Stress relaxation of H-shaped $A_2-\mathbf{A}-A_2$ polymers, for example, is believed to be initially dominated by retraction dynamics of dangling arms.[3] During this time period the backbone or cross-bar connector (**A**) remains virtually immobile, providing minimal contribution to stress relaxation dynamics. After relaxation of the arms is complete, both ends (branch points) of the backbone become mobile, but are not free from friction produced by these relaxed arms. These movable branch points enable the backbone to behave like a linear chain moving against frictional drag concentrated at the ends. Thus, terminal relaxation dynamics of branched architectures are believed to be controlled by reptation diffusion of backbone segments at long times.[3−6] Though this sequence qualitatively matches experimental observations, it has been found that an empirical expression for the branch point diffusivity $D_{bp} = (p a(\phi_{bb}))^2/2q\tau_a$, is needed to properly describe experimental linear viscoelastic data, particularly at low oscillation frequencies. Here q is the number of arms per branch point; τ_a is the arm retraction time; ϕ_{bb} is the volume fraction of backbone (or cross-bar) segments; $a(\phi_{bb}) = a_0/\phi_{bb}^{2/3}$ is the diluted tube diameter based on the original tube diameter a_0 and the dilution exponent under the Θ condition $\alpha = {}^4/_3$; and p is the unknown fraction of a tube diameter the branch point moves in a time of order $q\tau_a$. The value of p, for example, is expected to be unity, if a branch point hops a distance of order the fully dilated tube diameter, $a(\phi_{bb})$, in a time τ_a. On the other hand, if the motion of the branch point is heavily restricted by entanglements among the attached arms, p^2 is small and the branch point can be regarded as essentially pinned in space on time scales shorter than the terminal time of the entire molecule. This means that arm retraction dynamics can successfully compete with reptation diffusion for relaxing stress in the arms.

For H-shaped melts, a fixed p^2 value of ${}^1/_6$ was reported by McLeish et al.,[3] while for multiarm $A_3-\mathbf{A}-A_3$ melts p^2 was found to vary from ${}^1/_6$ to ${}^1/_{26}$, depending on the arm and backbone molecular weight.[5] Furthermore, in solutions of multiarm polymers, p^2 was recently reported to increase with decreasing polymer volume fraction ϕ as $p^2 \sim \phi^{-4/3}$.[6] These results clearly show that terminal dynamics in branched polymers are more complicated than suggested by strictly hierarchical models for stress relaxation. Much of the complexity can be traced to incomplete understanding of dynamics of the branch point following arm retraction. This situation should be contrasted with the high degree of accuracy with which stress relaxation dynamics of entangled symmetric star polymers can be predicted by tube theories.

Gell et al.[8] used a series of poly(ethylene-*alt*-propylene)(PEP) three-arm asymmetric stars (A−B−A) with variable B arm length to determine the critical branch length required for the transition from linear-like to dominant starlike terminal relaxation dynamics. These authors compared the zero-shear viscosity and self-diffusion coefficients for materials with varying degrees of arm length asymmetry and observed that rather short arms, with as little as two entanglements per arm, are sufficient to produce starlike dynamics in asymmetric star molecules. This result has recently been confirmed by Frischknecht et al.,[9] who studied relaxation dynamics in a series of 1,4-polyisoprene (PI) asymmetric three-

10.1021/ma047687i CCC: $30.25
Published on Web 04/19/2005

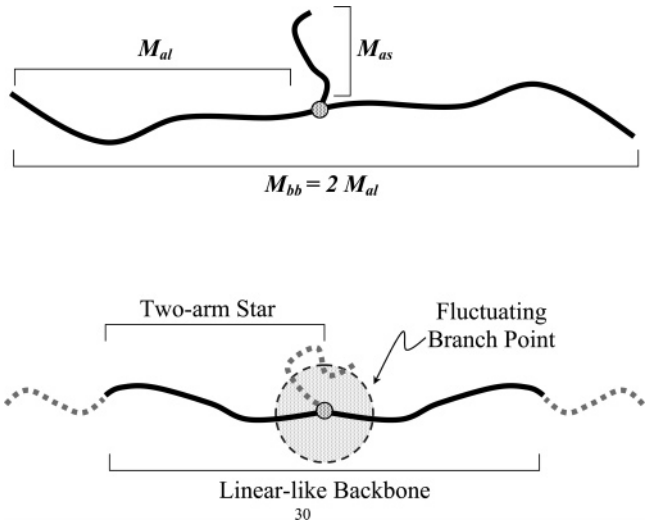

Figure 1. Schematic illustration for the asymmetric three-arm star polymer. (a) Asymmetric star polymer with a short arm M_{as} and two equal-length of long arms M_{al} of which the initial backbone molecular weight is $M_{bb} = 2M_{al}$. (b) Asymmetric star polymer as a remaining linear-like backbone with the branch-point after the relaxation of the short arm.

arm stars with short arm (B) entanglement densities varying from 2 to 9. These authors observed starlike relaxation spectra even for asymmetric star polymers with the smallest short arm length.

Frischknecht et al.[9] also developed a theory for stress relaxation dynamics of asymmetric polymers based on the assumption that the relaxation dynamics of these materials are hierarchical. The theory considered several possibilities for the motion of a branch point: (1) reptation of the backbone in a dilated tube accompanied by branch point hopping in the primitive, undilated tube; (2) reptation of backbone in a dilated tube accompanied by branch point motion also in a dilated tube. In either case, the branch point diffusivity can be written as $D_{bp} = p^2 a_{eff}^2/2\tau_a$, where in case 1 $a_{eff} = a_0$ and in case 2 $a_{eff} = a_0/\phi_{bb}^{2/3}$. Frischknecht et al. found their experimental results were best-fit by p^2 values in the range 1 to $^1/_{40}$, under the assumption of case 1, and by p^2 values from $^1/_4$ to 1/60, in case 2, as the length of the short arm (B) decreases. However, the observed trend of p^2 values according to short arm length is quite counterintuitive because smaller short arm causes more friction for branch point to diffuse along the linear-like backbone.

In view of the prominence of starlike dynamics in asymmetric star polymers studied by Gell et al.[8] and Frischknecht et al.,[9] it is useful to ask the following question: What is the relationship between the motion of branch point and polymer architecture? In other words, how can structural effects be incorporated into theories for relaxation dynamics of branched molecules without introducing new parameters for dealing with motion of branch points? To answer this question, we will conduct a detailed study of stress relaxation dynamics of asymmetric star 1,4-polyisoprene with the architecture depicted in Figure 1. In this case, we will hold the short arm entanglement density M_{as}/M_e fixed and vary the molecular weight of the long arm. The advantage of this asymmetric star system is two-fold: First, any ambiguity about the state of entanglement of the short arm can be removed by choosing the short arm molecular weight to be large enough (here 7 M_e); and second, because the branch point is positioned at

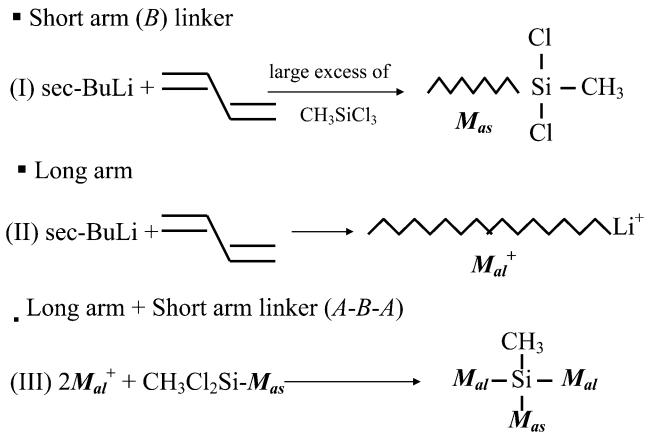

Figure 2. Schematic methodology to synthesize A−B−A architectures. (I) Synthesis of short arm linkers B with CH_3SiCl_3. (II) Synthesis of living long arms *A*. (III) Branching reaction between short arm linkers and living long arms: A−B−A architecture.

the center of a linear-like backbone, the conditions required for free reptation of the linear backbone can be systematically studied by varying the long arm molecular weight.

2. Experimental Section

A symmetric and three asymmetric 1,4-polyisoprene (PI) star polymers were synthesized using anionic techniques under high vacuum conditions. PI polymerization was carried out using degassed cyclohexane and isoprene monomer, which were purified by *n*-butyllithium prior to distillation to the reaction vessel. At ambient temperature, *sec*-butyllithium was used as the initiator. Methyl trichlorosilane (CH_3SiCl_3) was purified by distillation into an ampule after degassing. To obtain asymmetric star polymers with an A−B−A architecture, the living short arm B is first added to a large excess of purified CH_3SiCl_3 to produce a CH_3SiBCl_2 linker. A roughly 100-times stoichiometric excess of CH_3SiCl_3 was added to the living short arms to reduce the possibility of more than one living arms attaching to the linker. Excess CH_3SiCl_3 was removed by direct vacuum distillation. The CH_3SiBCl_2 linker was subsequently added to a small stoichiometric excess of the living long arms (A) to form the desired asymmetric A−B−A star polymer. The synthesis scheme is shown in Figure 2.

The final linking reaction is carried out in a MBraun Labmaster glovebox, facilitating convenient addition or removal of materials during synthesis. To verify the desired structure is obtained the linking reaction was followed by periodically withdrawing samples and performing GPC analysis (see Figure 3). The position of the chromatogram peak at the higher elution volume is consistent with expectations for the initial short arm linker, while that of the peak at the lower elution volume coincides with expectations for the target asymmetric star architecture. It is clearly evident from the figure that the short arm linker is transformed to the A−B−A architecture via an A−B intermediate, indicating that branches add sequentially to the chlorosilane linking agent. The final asymmetric star polymers were separated from unreacted arms in the terminated crude product by repeated toluene/methanol fractionation. If short arm linkers (CH_3SiBCl_2) are added instead to an excess of living short arms (B), symmetric three-arm star polymers (B_3) can be synthesized in the same manner.

Molecular weights of all polymers used in this study were extensively characterized using a Viscotek size exclusion chromatography (SEC) comprised of 4 mixed-bed columns and equipped with a laser light scattering detector (TDA 302). The microstructures of the polymers were characterized using ^{1}H NMR analysis.[10] Characterization results are provided in Table 1. While the number of entanglements per short arm is fixed at $Z_B = M_B/M_e = 7$, the number of entanglements per backbone

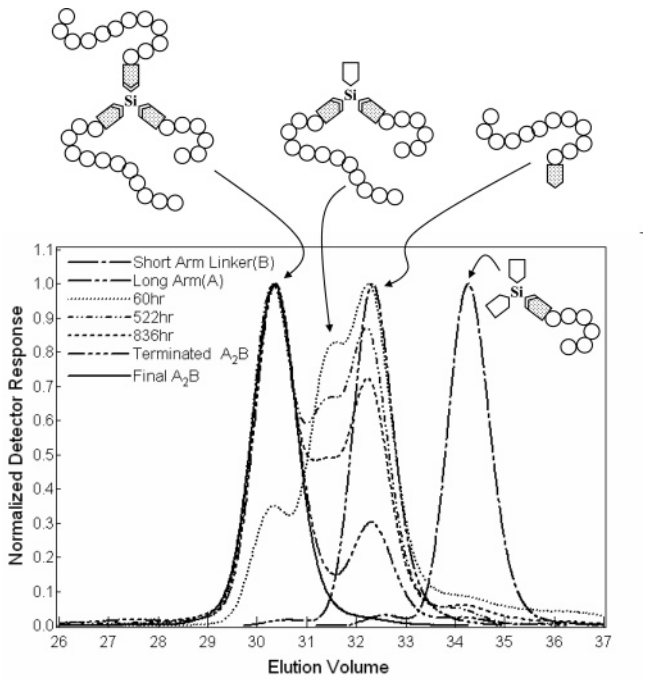

Figure 3. GPC analysis of samples taken during the branching reaction of asymmetric star polymers (A_2B73K).

strand $Z_A = M_A/M_e$ varies from 7 to 43, where $M_e = 4200$ g/mol.[11] An A_2B series polymer coded A_2BQK therefore has a fixed B-arm molecular weight $M_B = 33\,000$ g/mol and a variable A-arm molecular weight $M_A = Q \times 10^3$ g/mol.

Stress relaxation dynamics of asymmetric star polymers were quantified using small amplitude oscillatory shear measurements. A Rheometric Scientific Inc. (RSI) ARES-LS rheometer with 10 mm and 4 mm diameter parallel-plate fixtures was used for all experiments reported in this article. Linear viscoelastic properties of asymmetric stars were measured at temperatures ranging from −40 to +28 °C. In particular, the low-temperature experiments were performed with a 4 mm diameter parallel-plate to reduce torque compliance during measurement. The RSI Ochestrator software was used to automatically derive master curves at a reference temperature $T_{Ref} = 28$ °C by a two-dimensional residual minimization technique. The temperature-dependent shifting factors for the time and modulus scales (a_T and b_T) are provided in Figure 4. The WLF fit for the shift factor a_T, $\log(a_T) = [-C_1(T - T_{Ref})]/[C_2 + T - T_{Ref}]$, yields $C_1 = 4.8$ (±0.1) and $C_2 = 137$ (±3), which are similar to the values of $C_1 = 5.0$ and $C_2 = 140$ for asymmetric stars,[9] the values of $C_1 = 4.1$ and $C_2 = 122$ for linear polyisoprene,[12] and $C_1 = 4.5$ (±0.3) and $C_2 = 136$ (±6) for linear polyisoprene.[13] The values of b_T increase as temperature decreases. A similar trend for b_T was observed from linear polyisoprene.[13]

3. Results and Discussion

3.1. Linear Viscoelasticity of Asymmetric Stars. While repeated fractionations provide a mechanism for reducing undesirable byproducts of our synthesis, fractionation does not entirely eliminate these components. Figure 5a for example illustrates SEC chromatograms of a typical sample, A_2B182K, after the third and the final fractionation cycles. Although the polydispersity indices are small (1.09 and 1.02, respectively), there are small, but noticeable shoulders in both chromatograms. We therefore begin by examining the effect of these levels of impurities on the stress relaxation dynamics of asymmetric star polyisoprenes. Figure 5b depicts storage and loss moduli for the two materials in Figure 5a. It is apparent from the figure that while there are small quantitative differences between the two pairs of curves, the shapes of the plots are essentially identical. This implies that the dynamics of the prevailing architecture are strong enough to absorb contributions from the minor components. SEC chromatograms of the materials studied in the remainder of the article are depicted in Figure 5c. On the basis of the results in Figure 5b, we therefore anticipate that the viscoelastic properties of these materials are principally a reflection of the dynamics of the target asymmetric star structures.

Dynamic storage $G'(\omega)$ and loss $G''(\omega)$ moduli for a symmetric B_3 star (S33K) and three asymmetric star polymer melts (A_2B73K, A_2B124K, and A_2B182K), are plotted in Figure 6a. The lines in the figure are the storage and loss moduli data for a linear polyisoprene (N250K) with the similar microstructure as the branched molecules and nearly identical molecular weight as the backbone section (A_2-) of sample A_2B124K. Several qualitative characteristics of the $G'(\omega)$ and $G''(\omega)$ plots in Figure 6a are consistent with expectations for the targeted branched structures. The shape of the $G''(\omega)$ maximum at the intermediate frequencies (i.e. prior to the onset of terminal behavior) is clearly broader for the symmetric and asymmetric star polymers than for the linear PI. Also, the magnitude of the maximum is substantially lower for the branched polymers. Finally the relaxation spectrum for A_2B124K is substantially broader than that of N250K even though the backbone lengths and overall molecular weights of the two polymers are quite similar. All of these rheological features are consequences of greater retardation of molecular relaxation of the branched molecules due to the presence of the branch point.

It is possible to establish the qualitative effect of the *A* arms on stress relaxation behavior of asymmetric star polymers by comparing the shapes of $G'(\omega)$ and $G''(\omega)$ for molecules with fixed M_B and variable M_A (Figure 6a) and those with fixed M_A and variable M_B (Figure 6b). Figure 6b summarizes dynamic moduli for the *as*-series polymers studied by Frischknecht et al.[9] The qualitative similarity of $G'(\omega)$ and $G''(\omega)$ for the two asymmetric star series is readily apparent from the figures. It is also evident from the plots that increase in either M_A or M_B broadens the $G''(\omega)$ maximum and reduces its prominence. In other words increasing M_A or M_B favors more starlike dynamics. This result is at odds with expectations from strictly hierarchical models for branched polymer dynamics, which contend that after relaxation of the B-arm the linear-like A-arm relaxes by reptation diffusion. Thus, as M_A is increased at fixed M_B we would expect a stronger signature of linear-like, as opposed to the observed increasing starlike, dynamics at intermediate and low oscillation frequencies. More careful scrutiny of the *as*-series data (Figure 6b) indicates that both the magnitude and position of the $G''(\omega)$ maximum is independent of the overall polymer molecular weight. Thus, the $G''(\omega)$ maximum is primarily a reflection of dynamics during the early stage of the retraction of the A-arms.

Figure 7 illustrates the effect of M_A on the terminal properties of the A_2B series polymers. The zero-shear viscosity $\eta_0 \equiv G''(\omega)/\omega|_{\lim\ \omega\to 0}$ is obtained directly from the oscillatory shear data. Two approaches are used to estimate the terminal relaxation time. The first approach identifies τ with the oscillation frequency ω_c at which $G'(\omega)$ and $G''(\omega)$ crossover prior to the onset of

Table 1. Molecular Characterization

sample	M_n (SEC with LS) (g/mol) (1) short (2) long (3) total	PDI	microstructure by ^{1}H NMR (%) (1)*cis*−1,4 (2)*trans*−1,4 (3) 3,4	η_0 (Pa s)	$\omega_{cross-over}$ (1/s)	$\omega_{\eta''max}$ (1/s)	M in model (g/mol) (1) short (2) long
S33K	(1) 33 000	1.01	(1) 71.2	8.33×10^3	3.46×10	1.48×10	(1) 32 000
	(2)		(2) 21.7				(2) 33 000
	(3) 96 400	1.02	(3) 7.1				
A_2B73K	(1) 33 000	1.01	(1) 71.5	2.91×10^5	5.75×10^{-1}	1.59×10^{-1}	(1) 33 000
	(2) 73 400	1.05	(2) 21.4				(2) 73 400
	(3) 169 000	1.06	(3) 7.1				
A_2B124K	(1) 33 000	1.01	(1) 72.9	1.35×10^7	5.22×10^{-3}	2.22×10^{-3}	(1) 33 000
	(2) 124 000	1.03	(2) 19.9				(2) 124 000
	(3) 277 000	1.04	(3) 7.2				
A_2B182K	(1) 33 000	1.01	(1) 73.1	1.68×10^8	3.57×10^{-4}	2.28×10^{-4}	(1) 33 000
	(2) 182 000	1.06	(2) 18.9				(2) 182 000
	(3) 370 000	1.02	(3) 8.0				
N250K	(1)		(1) 74.4				(1) 1000
	(2)		(2) 19.8				(2) 128 450
	(3) 256 900	1.01	(3) 5.8				

terminal behavior. In the second approach, τ is designated as the reciprocal of the frequency $\omega_{\eta''max}$ at which $\eta''(\omega) \equiv G'(\omega)/\omega$ manifests a local maximum. It is apparent from Figure 7 that terminal properties manifest power-law dependences on M_A. The power-law exponents are clearly quite large, which is consistent with expectations for dominant starlike polymer dynamics in the terminal regime.

Another characteristic feature of stress relaxation of asymmetric star polymers is the inflection in the loss modulus at low frequencies. The inflection appears to coincide with a change in the underlying molecular relaxation dynamics and is reminiscent of the loss behavior of entangled solutions of linear polymers in the plateau regime. In the case of the A_2B-series, the inflection becomes more pronounced as M_A is increased, while for the *as*-series materials it becomes more detectable as M_B is reduced. Introducing an asymmetry factor $\beta \equiv (M_A - M_B)/M_A$, we can now say that for starlike asymmetric stars, such as A_2B73K and as37 for which $\beta = 0.55$ and 0.64, respectively, the inflection is virtually nonexistent and the overall shape of $G''(\omega)$ is similar to that of a symmetric star. On the other hand, for highly asymmetric polymers such as as11 ($\beta = 0.89$) and A_2B182K ($\beta = 0.82$), the inflection is prominent and the overall shape of $G''(\omega)$ can be tentatively described as a combination of dominantly starlike behavior at high frequencies and weakly linear solution-like behavior at low frequencies.

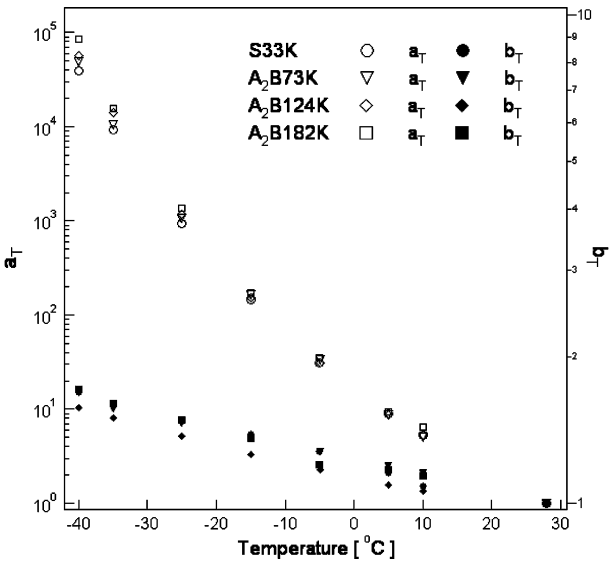

Figure 4. Temperature-dependent shifting factors a_T and b_T (T_{ref} = 28 °C) for a symmetric and three asymmetric star polymers.

The two apparently contradictory conclusions that follow from our discussion above (more dominantly starlike dynamics for asymmetric star polymers with high M_A or M_B, and a noticeable transition to solution-like terminal dynamics for polymers with large β) suggest a dual role of the long arms in stress relaxation of asymmetric star polymers. Specifically, while the latter observation is arguably consistent with a hierarchical relaxation scheme premised on starlike retraction dynamics of all arms on time scales $t < \tau_{a,B}$ and reptation-like dynamics of the unrelaxed linear segments on time scales $t \gg \tau_{a,B}$, the former observation is not. However, if in addition to their contribution to early starlike dynamics, the long arms also play a role in delaying the ultimate transition to reptation behavior, the two observations can be reconciled.

Following Frischknecht et al.[9] we write the friction coefficient of a branch point as

$$\zeta_{bp} = \frac{kT}{D_{bp}} = \left[\frac{2kT\tau_{a,B}}{a_{eff}^2}\right](p^{-2}) \qquad (1)$$

The first term in square brackets is the branch point friction coefficient for a symmetric star polymer with arm retraction time $\tau_{a,B}$. Assuming a_{eff} is known, the second term in eq 1 then reflects the extra resistance due to the asymmetry of the branch (segments belonging to the linear backbone are unrelaxed, while those belonging to the short arm are fully relaxed). On physical grounds we might guess that this extra resistance is a function of the number of entanglement segments of the long-arm that remain unrelaxed on the time scale $\tau_{a,B}$. For example, if the usual cartoon representation of the reptation tube as a cylinder with a circular cross-section is accepted, the unrelaxed long-arms will only cease to have an effect on branch point dynamics when their random coil size is just small enough that these coils can fit, unperturbed, into the effective tube constraining the branch point. This condition implies that to leading order the *degree of fit* (i.e., the ratio of the projected coil size to the tube cross-section area) determines the extra resistance the branch

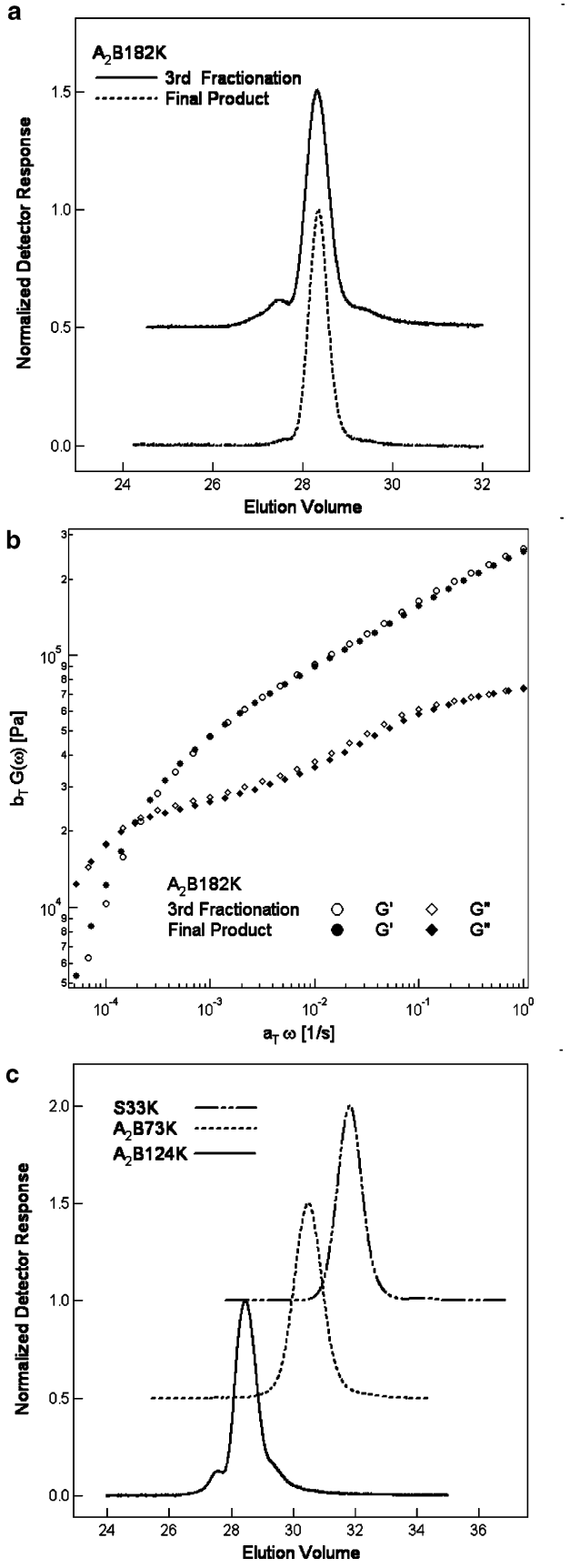

Figure 5. (a) GPC analysis of asymmetric star polymers (A_2B182K) taken from the 3rd and the final stage of fractionations. (b) Dynamic moduli, $G'(\omega)$ and $G''(\omega)$, of asymmetric star polymers (A_2B182K) taken from the 3rd and the final stage of fractionations. (c). GPC analysis of symmetric and asymmetric star polymers (S33K, A_2B73K, and A_2B124K) taken from the final stage of fractionations.

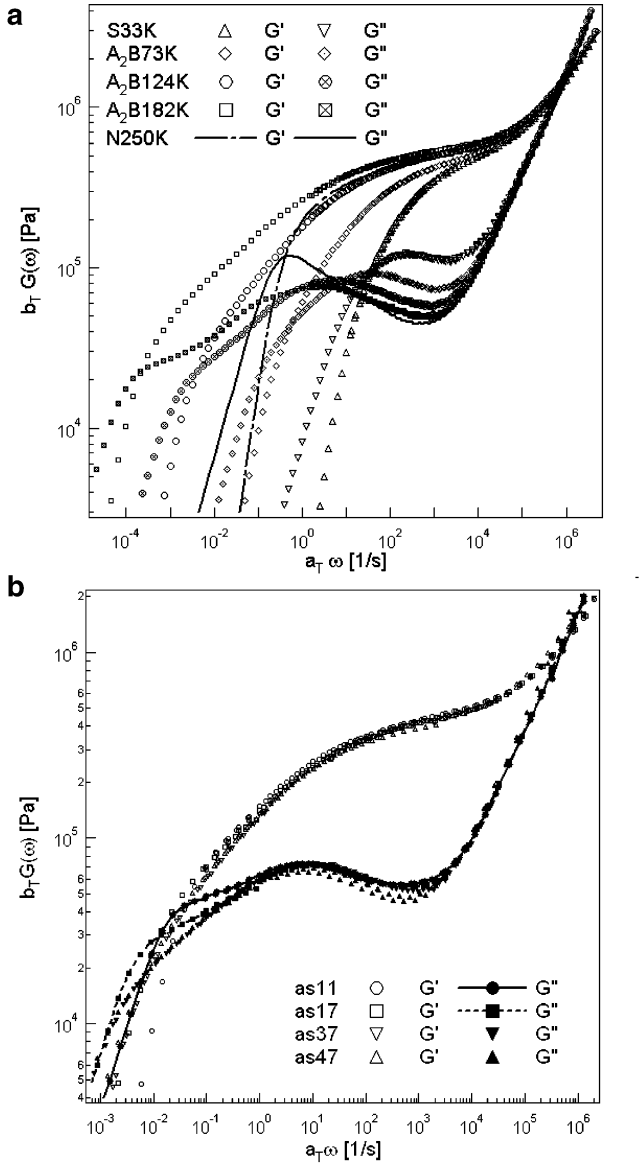

Figure 6. (a) Dynamic moduli, $G'(\omega)$ and $Gs''(\omega)$ of a symmetric and three asymmetric star polymers with linear polymers. The reference temperature is T_{ref} = 28 °C. (b) Dynamic moduli, $G'(\omega)$ and $G''(\omega)$ of asymmetric star polymers (*as*-series) reported by Frischknecht et al.[9] The reference temperature is T_{ref} = 25 °C.

point experiences. It then follows that $p^{-2} \propto (R_{AR}^2/a_{eff}^2) \sim (N_{AR}/N_{e,eff})$, where $N_{e,eff}$ is the effective entanglement molecular weight of a tube segment at times $t \geq \tau_{a,B}$.

3.2. Theory. The theory of Frischknecht et al.[9] provides a good starting point for modeling stress relaxation and linear viscoelastic response of asymmetric star polymers. The main assumptions are that relaxation dynamics are hierarchical and that relaxed segments dilate the entanglement structure in which unrelaxed segments diffuse. Thus, on time scales shorter than the entanglement Rouse time τ_e, relaxation begins with free Rouse motion at the arm extremities. This is followed by retraction of the short and long arms with appropriate accounting for differences in dilution dynamics of the more slowly relaxing long-arm and relatively faster relaxing short-arm segments. After the relaxation of short arm, the model contends that dynamics of an asymmetric star polymer should be similar to those of a linear polymer with molecular weight

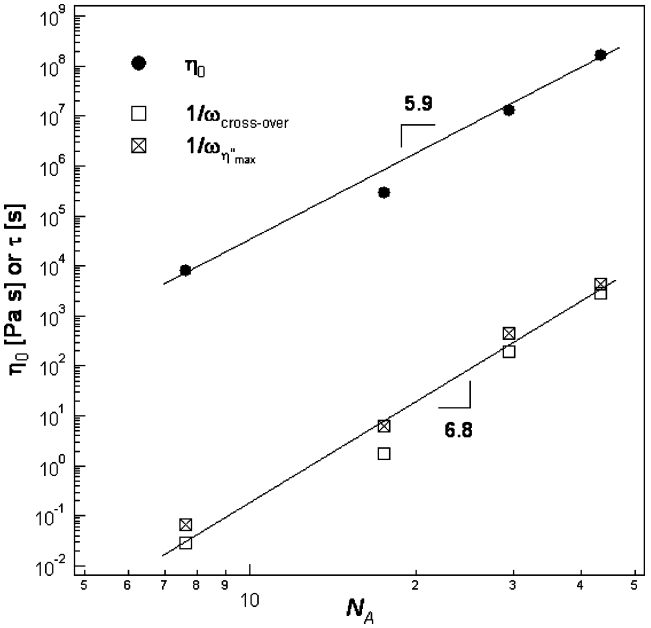

Figure 7. Dependence of terminal properties, the zero-shear viscosity, and the terminal relaxation times on the long arm length of symmetric and asymmetric star polymers

$2M_{AR}$, rather $2M_A$,[9] where M_{AR} is the unknown molecular weight of the section of the long arms that is unrelaxed on a time scale $\tau_{a,B}$. Shallow retractions due to contour length fluctuations followed by reptative motion would therefore be expected to compete with deeper arm retraction for relieving stress in the long arms following relaxation of the short arms.

On the basis of the well-known exponential dependence of arm retraction time on the degree of entanglement of long arm, reptation diffusion is anticipated to provide a more efficient mechanism for relaxing stress in asymmetric star polymers on time scales $t > \tau_{a,B}$. To account for the influence of the short arm on reptation of the unrelaxed linear-like backbone, Frischknecht et al.[9] assumed that the rate of reptation diffusion of the backbone is inversely proportional to the effective total drag produced by the short arm as well as the Rouse friction acting on the backbone. Thus, the effective diffusivity, D_{eff}, is

$$1/D_{eff} = 1/D_{bp} + 1/D_c \tag{2}$$

where D_{bp} is the branch point diffusion constant along the tube enmeshing backbone segments and $D_c = k_BT/2N_{AR}\zeta_0$ is the Rouse diffusion constant from backbone monomers. Here $N_{AR} = M_{AR}/m_0$ is the number of (Kuhn) monomers in the unrelaxed backbone; m_0 and ζ_0 are the monomer molecular weight and friction coefficient, respectively. The branch point diffusivity is formulated as $D_{bp} = (pa_{eff})^2/2\tau_{a,B}$ under the assumption that the branch point hops a distance of order the tube diameter (pa_{eff}) after each cycle of short arm retraction. If the dynamic dilution principle is applied uniformly to all sections of the chain, a_{eff} is the dilated tube diameter, enlarged by lost entanglements due to relaxed short-arm and long-arm segments. There is nonetheless some evidence that the appropriate choice for branched polymers is a_{eff} equal to the undilated or original tube diameter $a_0 = \sqrt{N_e}b$.[6,14] The variable p is an adjustable parameter designed to absorb uncertainty about the amplitude of branch point hops and $N_e = M_e/m_0 = a_0^2/b^2$ is the number of (Kuhn) monomers of contour length b in an entanglement strand. The terminal relaxation time of an asymmetric star polymer is then taken to be the time when reptation of the linear-like backbone $\tau_d(s)$ becomes faster than the time required for deep retractions $\tau_A(s)$ of long arm segments. Thus, reptation will occur at a time $\tau_d(s) = \tau_A(s)$ set by competition between reptation diffusion and arm retraction, where s is a fractional distance from the chain end.

The fraction $(1 - s_d)$ of backbone segments that will relax by reptation is then obtained from the crossover between these two time scales, i.e., from the expression $\tau_d(s_d) = \tau_A(s_d)$. Writing the effective contour length of backbone as $L_{eff} = (2N_{AR})b^2/a_{eff}$ and assuming $a_{eff} = a_0/\phi_{bb}^{\alpha/2}$ (i.e. uniform dilation) the reptation time for the unrelaxed backbone segments is given by

$$\tau_d = \tau_d(s_d) = \frac{L_{eff}^2(1-s_d)^2}{\pi^2 D_{eff}} = 3\left(\frac{2N_{AR}}{N_e}\right)^3 (1 - s_d)^2\tau_e\phi_{Rbb}^{\alpha}\left[1 + \frac{2}{3\pi^2 p^2(2N_{AR}/N_e)}\frac{\tau_{a,B}}{\tau_e}\phi_{Rbb}^{\alpha}\right] \tag{3}$$

where ϕ_{Rbb} is the volume fraction of unrelaxed backbone segments on time scales $t \geq \tau_{a,B}$ and $\alpha = 4/3$ is the dilution exponent for the polymer in a Θ solvent. Conversely, if we assume that the branch point diffuses in the undilated tube ($a_{eff} = a_0$), the terminal reptation time is

$$\tau_d = \frac{L_{eff}^2(1-s_d)^2}{\pi^2 D_{eff}} = 3\left(\frac{2N_{AR}}{N_e}\right)^3 (1 - s_d)^2\tau_e\phi_{Rbb}^{\alpha}\left[1 + \frac{2}{3\pi^2 p^2(2N_{AR}/N_e)}\frac{\tau_{a,B}}{\tau_e}\right] \tag{4}$$

As discussed in the Introduction, a serious shortcoming of this theory is that the variable p must be adjusted arbitrarily to fit experimental data.[9] Here we wish to derive an analytical formula for this variable that is consistent with the physics outlined earlier. We will also demand that the chosen formula facilitates smooth crossover of eqs 3 and 4 to the linear-like and starlike limiting cases. To begin we consider the case of an "almost linear" asymmetric star polymer with $N_{AR} \gg N_e$, $N_B \approx O(N_e)$. In this case, $\beta \approx 1$, and it is easy to show that the terminal reptation time predicted by eqs 3 and 4 is close to the expected result for a linear chain, $\tau_d = 3(2N_{AR}/N_e)^3(1 - s_d)^2\tau_e$, if $p^2 = (2N_{AR}/N_e)^{-1}$. Next consider the case, $N_A \approx N_B$ and $2N_{AR} \approx O(N_e)$. In this case the asymmetry factor β is close to zero, long arm segments are almost relaxed (i.e. $\phi_{Rbb} \approx 0$) so the expected terminal reptation process is not effective. Therefore, the terminal relaxation time is anticipated as $\tau_{terminal} = L_{eff}^2/D_{eff} = a_{eff}^2/D_{eff} = a_{eff}^2[2\tau_{a,B}/p^2a_{eff}^2 + 2N_{AR}/k_BT] \approx \tau_{a,B}/p^2$. Taking $p^2 = (2N_{AR}/N_e)^{-1}$, this reduces to the expected result $\tau_{terminal} \approx \tau_{a,B}$.

We therefore conclude that if eqs 3 or 4 is to be uniformly valid at all β,

$$p^2 = (2N_{AR}/N_e)^{-1} = \frac{1}{(2N_{AR})b^2/a_{eff^*}^2} \tag{5}$$

Here a_{eff^*} is the effective tube diameter realized by segments in the unrelaxed remaining long arms, which is not necessarily same to the effective tube diameter

immediately after the relaxation of short arm. This result is close to the approximate result deduced in the previous section by purely physical arguments. Substituting for p^2 in eq 1 we obtain $D_{bp} = 1/[(2N_{AR})b^2/a_{eff*}^2]$-$(a_{eff}^2/2\tau_{a,B})$, confirming that the branch point diffusivity of an asymmetric star polymer can indeed be interpreted as regular starlike diffusive motion of a branch point $a_{eff}^2/2\tau_{a,B}$ retarded by an effective drag, $p^2 = 1/[(2N_{AR})$-$b^2/a_{eff*}^2]$, produced by unrelaxed backbone segments.

A perhaps obvious question is can eq 5 account for the puzzling trend of p^2 values reported by Frischknecht et al.[9] for their as-series polymers. Recall that in the as-series polymers the molecular weight of the long arms, M_A, is held fixed and M_B is varied from $2M_e$ to $9M_e$. The number of unrelaxed long-arm segments N_{AR} at time $t \approx \tau_{a,B}$, is therefore anticipated to increase as the molecular weight of the short arm is progressively reduced. By eq 5, p^2 should therefore decrease as M_B is lowered toward $2M_e$, which is consistent with the observations of Frischknecht et al.,[9] at least qualitatively. Quantitative comparisons are possible, but require a relationship between N_{AR} and N_B for the *as*-series polymers. Because the more slowly relaxing long arms will exert a nontrivial effect on short-arm relaxation, and vice versa, it is not possible to derive this relationship in analytical form. We therefore turn to comparisons of the experimental $G'(\omega)$ and $G''(\omega)$ data with numerical predictions based on the theory of Frischknecht et al.,[9] with the branch point retardation coefficient given by eq 5.

The physical assumptions and mathematical equations used in these comparisons are detailed in the Appendix. The equations are similar to those proposed by Frischknecht et al.,[9] but numerical factors have all been corrected according to Likhtman and McLeish.[15] At early times ($\tau_e < t < \tau_{a,B}$), the short arm and long arms undergo arm retraction and dynamics are qualitatively similar to a blend of two star polymers. In this regime, the relaxation time of the short arm, $\tau_{B,b}$ (s_B) and long arm $\tau_{A,b}(s_A)$ are expressed in terms of the fractional distance from the arm end s_i. Here, subscripts i indicate short arms (i = B) and long arms (i = A). The relaxed fraction of long arm s_{AR} at the completion of short arm retraction is determined by solving for $\tau_{B,b}$-$(s_B = 1) = \tau_{a,B} = \tau_{A,b}(s_{AR})$. Then, the remaining long arm length is $N_{AR} = N_A(1 - s_{AR})$ and the unrelaxed fraction of long-arm segments becomes $\phi_{Rbb} = [2M_A(1 - s_{AR})]/(M_B + 2M_A)$, compared to the initial long arm volume fraction, $\phi_{bb} = \phi_A = 2M_A/(M_B + 2M_A)$. At this time, the effective fraction of unrelaxed segments of long arms changes abruptly leading to a constraint-release (CR) Rouse process on time scales τ_C where the long-arm equilibrates in the dilated tube.[16] Further relaxation, after τ_C, proceeds by arm retraction of unrelaxed long arm segments with characteristic time $\tau_A(s_A)$ in the dilated network. The final stage of stress relaxation is determined by a competition between arm retraction and reptation diffusion of the linear-like fragment (backbone) of unrelaxed long arms.

While the fundamental time scale for each branch point hop during the terminal reptation process is known to be $\tau_{a,B}$, the distance the branch-point can move in this time remains controversial. Recent experimental and theoretical studies[6,11,17] suggest that slower relaxing (unrelaxed) segments may not always be able to take full advantage of the perforated entanglement environment provided by faster relaxing segments (or chains) for further relaxations. For simplicity, we here consider two simple but extreme cases. (I) Undilated tube hopping with undilated entanglement resistance (UHUR): In this case the tube diameter accessible to the branch point is not affected by the relaxed chain segments and $a_{eff} = a_{eff*} = a_0$. (II) Dilated tube hopping with dilated entanglement resistance (DHDR): In this case $a_{eff} = a_{eff*} = a_0/\phi_{Rbb}^{\alpha/2}$. The terminal or reptation time is then given by

$$\tau_d = \frac{L_{eff}^2(1 - s_d)^2}{\pi^2 D_{eff}} =$$

$$\begin{cases} 3\left(\frac{2N_{AR}}{N_e}\right)^3(1 - s_d)^2\tau_e\phi_{Rbb}^{\alpha}\left[1 + \frac{2}{3\pi^2}\frac{\tau_{a,B}}{\tau_e}\right] & \text{(6I)} \\ 3\left(\frac{2N_{AR}}{N_e}\right)^3(1 - s_d)^2\tau_e\phi_{Rbb}^{\alpha}\left[1 + \frac{2}{3\pi^2}\frac{\tau_{a,B}}{\tau_e}\phi_{Rbb}^{2\alpha}\right] & \text{(6II)} \end{cases}$$

3.3. Comparisons between Experiment and Theory. The plateau modulus, $G_I = 0.45(\pm 0.06)$ MPa, of the A_2B-series polymers is estimated as the average storage modulus value at which the first rubbery loss minimum is observed. This leads to an entanglement molecular weight $M_e = \rho RT/G_e = \rho RT/[(5/4)G_I] = 4004$ g/mol, where we use the literature value of the density of PI, $\rho = 0.9$ g/cm^3,[18] and reference temperature $T_{Ref} = 301$ K. While the model parameter for time scale, $\tau_e = \zeta_0 a^4/3\pi^2 k_B T b^2$, can be calculated from measured or literature values, data for some parameters, e.g., ζ_0, are not generally available at the condition used for the experiments. Thus, the value of τ_e is obtained by fitting the model expression to the measured dynamic moduli in the high-frequency Rouse regime. This shifting along the frequency axis yields the best-fit entanglement equilibration time $\tau_{ef} = 7.4 \times 10^{-6}$ s. Using the evaluated model parameters (i.e. $G_I = 0.45$ MPa, $M_e = 4004$ g/mol, and $\tau_{ef} = 7.4 \times 10^{-6}$ s). We next compare theoretical predictions and experimental $G'(\omega)$ and $G''(\omega)$ data for the A_2B-series asymmetric star polymers. Results are provided in Figure 8a−c for all polymers used in the study. Unlike earlier work,[9] the amplitude of a branch point hop is obtained self-consistently using eq 5.

It is immediately evident from the figures that most features of the experimental data are correctly captured by the theory. Qualitative changes in the shape of $G'(\omega)$ and $G''(\omega)$ with increasing polymer length asymmetry, β, are also correctly captured by the theory. It is apparent that the DHDR mode produces faster relaxation than the UHUR mode. Predictions based on the UHUR model are generally in better agreement with the data in the low-frequency, terminal regime, while those underestimate $G'(\omega)$ and $G''(\omega)$ in the intermediate and high frequencies. The overall quality of the comparisons therefore does not strongly favor either of the two versions of the model. We nonetheless recognize that since the UHUD and DHDR modes are simplified extremes, it is plausible that an intermediate case (e.g. UHDR) may apply and that even a transition from UHUD mode to DHDR mode relaxation can occur. These details are obviously important, but are not the focus of the present study. We leave them up to the theorists to resolve.

Figure 9a−c compares the theory with previously published $G'(\omega)$ and $G''(\omega)$ data for the *as*-series polymers.[9] For simplicity, we only focus on predictions of

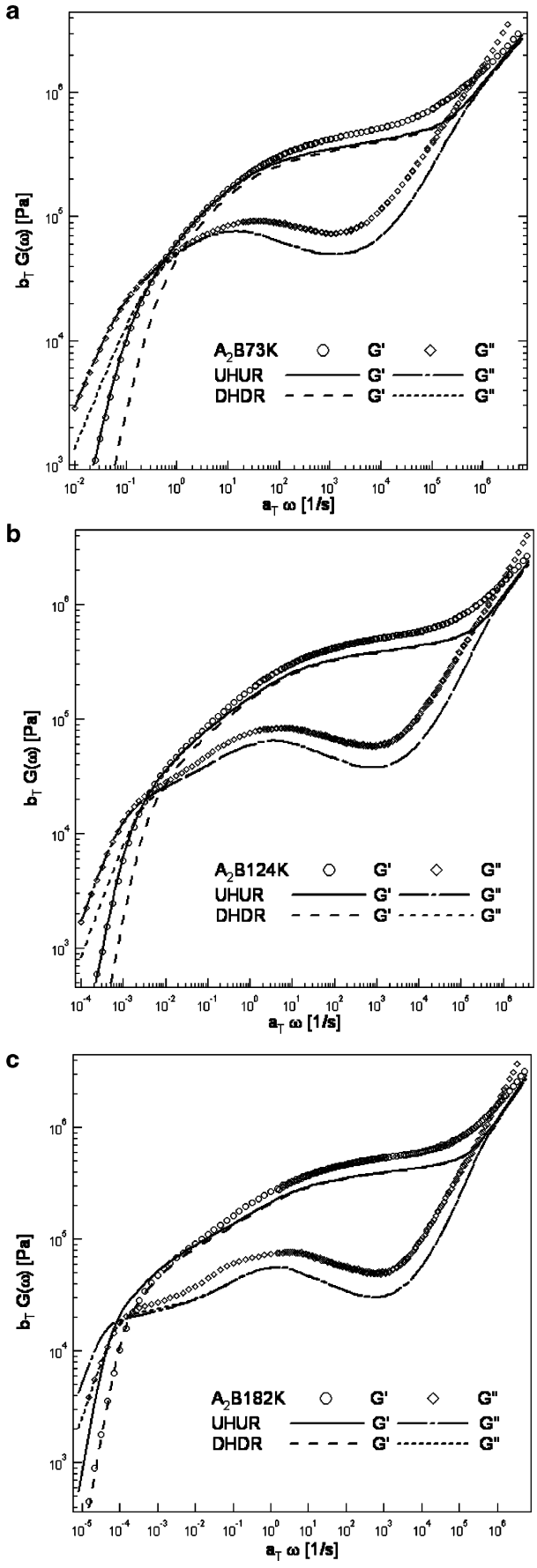

Figure 8. Comparison of experimental and theoretical moduli, $G'(\omega)$ and $G''(\omega)$, of (a) A_2B73K, (b) A_2B124K, and (c) A_2B182K. The symbols are the measured data at $T_{ref} = 28$ °C and the lines are the model predictions with $G_I = 0.45$ MPa, $M_e = 4004$ g/mol, and $\tau_{ef} = 7.4 \times 10^{-6}$ s.

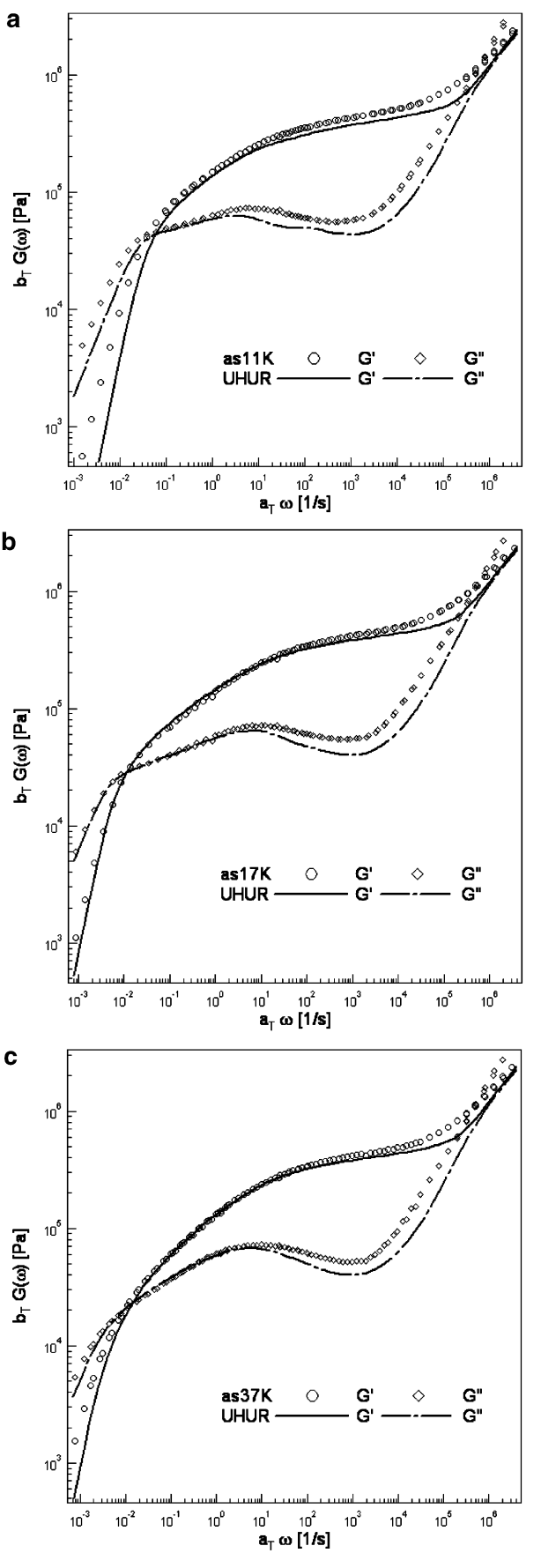

Figure 9. Comparison of experimental and theoretical moduli, $G'(\omega)$ and $G''(\omega)$, of (a) as11, (b) as17, and (c) as37. The symbols are the measured data reported by Frischknecht et al.[9] at $T_{ref} = 25$ °C and the lines are the model predictions with $G_I = 0.45$ MPa, $M_e = 4004$ g/mol, and $\tau_{ef} = 7.4 \times 10^{-6}$ s.

the UHUR version of the theory. The molecular weights of the long and short arms reported in ref 9 are used in the analysis and the same model parameters used for the A_2B-series (i.e. $G_I = 0.45$ MPa, $M_e = 4004$ g/mol, and $\tau_{ef} = 7.4 \times 10^{-6}$ s) are used throughout. Again, the p^2 variable is computed self-consistently using eq 5. Figure 9a−c show the theoretical predictions are in reasonably good agreement with the experimental results, but the agreement is not quantitative. The qualitative effect of arm length asymmetry on relaxation dynamics is again well reproduced by the theory. As was the case of the A_2B-series polymers, $G'(\omega)$ and $G''(\omega)$ of the *as*-series materials are underestimated at intermediate frequencies and the shape of the high-frequency regime is not accurately captured.

As discussed before, M_e can be computed from the experimentally measured plateau modulus G_I using the formula $M_e = \rho RT/[(5/4)G_I]$.[15] The accuracy of this M_e is then determined by the quality of the G_I value. Alternatively, both the plateau modulus and entanglement molecular weights can be treated as "model" parameters, obtained by fitting a model to experimental data.[11] Using the latter approach we obtain best-fit values $G_{Nf} = 0.6$ MPa and $M_{ef} = 4200$ g/mol from fits to linear and star PI melt data. M_{ef} is 5% larger than M_e, but G_{Nf} is 30% larger than G_I. It is evident from Figure 10a,b that the model predictions with G_{Nf} and M_{ef} are in better overall agreement with the data. $G'(\omega)$ and $G''(\omega)$ prior to the onset of terminal behaviors are, however, still overestimated. The terminal relaxation of asymmetric stars with larger N_A (e.g., A_2B182K) is better described by the model with the assumption that terminal relaxation occurs in the dilated tube. On the other hand, the majority of the other polymers such as A_2B73K with shorter N_A are well described by the undilated tube version of the model. These observations are probably related to the failure of tube dilation for symmetric stars reported by Watanabe.[17]

A simple estimate of the reptation time of remaining backbone in the dilated and undilated tube yields, $\tau_{CR,Rep}/\tau_{Rep} = \tau_{a,B}[2N_{AR}\phi_{Rbb}^{\alpha}/N_e]^2/\tau_e[2N_{AR}/N_e]^3$. On this basis one therefore concludes that terminal relaxation should always proceed in the undilated tube. The difficulty here is that there is a yet to be defined criterion by which unrelaxed sections of the chain chooses between the undilated and dilated tube. Also, the need for independently fitting the model parameters observed for all variants of the Milner−McLeish model,[2−7] even for narrow distribution linear melts,[15] is another problem to be settled. It is unclear whether all of quantitative discrepancies can be remedied by a more detailed exploration of the M_e and G_N relationship and/or intermediate possibilities for a_{eff^*}. However, at the level of the comparisons pursued here, we conclude that the theory proposed in this work correctly captures most aspects of the relaxation behavior of entangled asymmetric star polymers.

4. Conclusion

Linear viscoelastic behavior of a series of 1,4-polyisoprene asymmetric star polymers was investigated experimentally and theoretically in order to determine how branch point motion affects terminal relaxation dynamics. For the systems studied, the branch point is connected to a moderately entangled short arm ($M_B/M_e = 7$) and two longer arms with varying numbers of entanglements ($M_A/M_e = 7-43$). The degree of asymmetry in the given architectures $\beta = [(M_A - M_B)/M_A]$ varies from 0.55 to 0.82. We observe the measured loss modulus more sensitively reflects a transition in the governing dynamics as the asymmetry increases. This finding suggests a possibility that the governing dynamic transition can be described in terms of architecture.

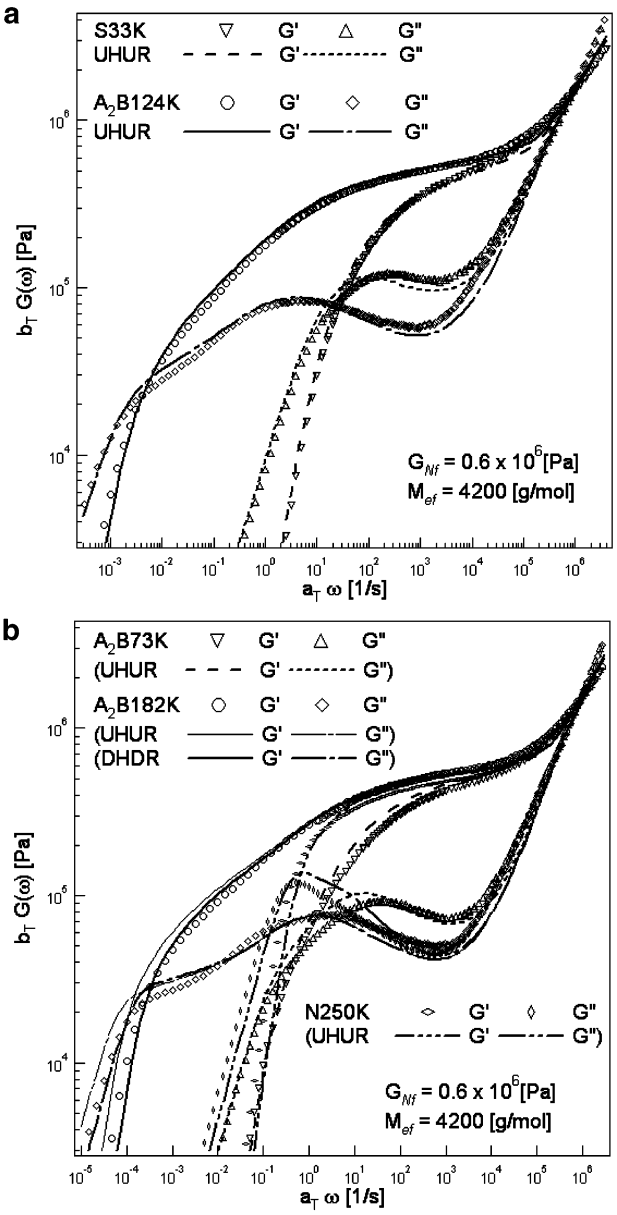

Figure 10. Comparison of experimental and theoretical moduli, $G'(\omega)$ and $G''(\omega)$, of (a) S33K ($s_d = 1$) and A_2B124K and (b) N250K, A_2B73K, and A_2B182K. The symbols are the measured data at $T_{ref} = 28$ °C, and the lines are the model predictions with $G_{Nf} = 0.6$ MPa, $M_{ef} = 4200$ g/mol and $\tau_{ef} = 7.4 \times 10^{-6}$ s.

A simple scaling approach provides a relationship $p^2 = 1/[(2N_{AR})b^2/a_{eff^*}^2]$ between the branch point hopping amplitude and the entanglement resistance produced by unrelaxed backbone segments. Model predictions using the proposed p^2 correctly capture most aspects of relaxation behaviors of asymmetric star polymers. However, our results do not provide definitive guidance on the tube environment in which terminal relaxation occurs. While the theory based on the undilated tube ansatz yields better agreement with experimental data for many of the asymmetric star polymers studied,

results for polymers with highest long-arm entanglement densities are in better accord with predications based on a dilated tube case.

Acknowledgment. The authors thank Amalie L. Frischknecht for the experimental data. Financial support from the National Science Foundation (Grant No. DMR0237052) and the Department of Energy Basic Science Program (Grant DE-FG02-02ER4600) are also gratefully acknowledged.

Appendix

The number of entanglement segments of long arm Z_A and short arm Z_B are defined as $Z_A = N_A/N_e = (M_A/m_0)/(M_e/m_0)$ and $Z_B = N_B/N_e = (M_B/m_0)/(M_e/m_0)$, respectively. s_i is the fractional distance from the end of arm, where subscripts i indicate long arms (i = A) and short arms (i = B). Also, the fraction of long arm ϕ_A and short arm ϕ_B are calculated as $\phi_A = 2M_A/(M_B + 2M_A)$ and $\phi_B = M_B/(M_B + 2M_A)$. The fraction of initial backbone is same to that of long arms ($\phi_{bb} = \phi_A$). After the free Rouse motion of all arm segments ($t > \tau_e$), the short and long arms undergo the arm retraction. In this regime, the effective fraction of unrelaxed segments $\Phi(s_i)$ and the effective potential $U_{i,b}(s_i)$ for short and long arms are defined as follows:

$$\Phi(s_A) = 1 - g_A s_A = 1 - \left(\phi_A + \phi_B\sqrt{\frac{Z_A}{Z_B}}\right)s_A \quad \text{(A-1)}$$

$$\Phi(s_B) = 1 - g_B s_B = 1 - \left(\phi_B + \phi_A\sqrt{\frac{Z_B}{Z_A}}\right)s_B \quad \text{(A-2)}$$

$$U_{i,b}(s_i) = 3Z_i\frac{1 - (1 - g_i s_i)^{\alpha+1}[1 + (1 + \alpha)g_i s_i]}{g_i^2(\alpha + 1)(\alpha + 2)} \quad \text{(A-3)}$$

Here, the effective fraction of unrelaxed segments $\Phi(s_i)$ is explicitly expressed in terms of the fractional distance s_i with the factor g_i derived from the Ball−McLeish equation.[9,16]

The *early fast diffusion* time and the *late diffusion* time of each arm are given by

$$\tau_{early}(s_i) = \frac{9\pi^3}{16}\tau_e Z_i^4 s_i^4 \quad \text{(A-4)}$$

$$\tau_{late}(s_i) = \sqrt{\frac{\pi^5}{6}}\tau_e Z_i^{3/2} \times \frac{\exp[U_{i,b}(s_i)]}{\sqrt{s_i^2(1 - g_i s_i)^{2\alpha} + \frac{1}{g_i^2}\left(\frac{g_i^2(1 + \alpha)}{3Z_i}\right)^{2\alpha/(1+\alpha)}\left(\Gamma\left[\frac{1}{(1 + \alpha)}\right]\right)^{-2}}} \quad \text{(A-5)}$$

The combined arm retraction time $\tau_{i,b}(s_i)$ is defined as

$$\tau_{i,b}(s_i) = \frac{\tau_{early}(s_i)\exp[U_{i,b}(s_i)]}{1 + \tau_{early}(s_i)\exp[U_{i,b}(s_i)]/\tau_{late}(s_i)} \quad \text{(A-6)}$$

After the relaxation of the short arm, the effective fraction of unrelaxed segments of long arms reduces from $\Phi(\tau_{a,B}) = \Phi(s_{AR}) = \phi_B(1 - s_{AR}\sqrt{Z_A/Z_B}) + \phi_A(1 - s_{AR})$ to $\phi_A(1 - s_{AR}) = \phi_{Rbb}$ so the constraint-release Rouse time τ_C is defined as $\tau_C = \tau_{a,B}[\Phi(\tau_{a,B})/\phi_{Rbb}]^{2\alpha}$ with $\Phi(t)^\alpha = \Phi(s_{AR})^\alpha\sqrt{\tau_{a,B}/t}$.[16] If relaxation of unrelaxed long arm segments is assumed frozen during the time when the constraint-release equilibrium is active, the remaining segments will recognize the increased entanglement spacing on a time scale of order τ_C. Therefore, further relaxation after τ_C will be governed by the dilated entanglement length $N_{e,D} = N_e/\phi_{bb}^\alpha$ and the diluted entanglement equilibrium time $\tau_{e,D} = \tau_e/\phi_{bb}^{2\alpha}$ with the number of entanglement segments of remaining long arm $Z_{A,D} = N_A/N_{e,D}$. The combined arm retraction time of long arm in the dilated tube $\tau_{A,DT}(s_i)$ can be expressed as $\tau_{A,DT}(s_i) = \{\tau_{early,DT}(s_i)\exp[U_{DT}(s_i)]\}/\{1 + \tau_{early,DT}(s_i)\exp[U_{DT}(s_i)]/\tau_{late,DT}(s_i)\}$, in analogy with eq A-6, from the diluted effective potential, the diluted *early* and *late diffusion* time.

$$U_{DT}(s_i) = 3Z_{A,D}\frac{1 - (1 - s_i)^{\alpha+1}[1 + (1 + \alpha)s_i]}{(\alpha + 1)(\alpha + 2)} \quad \text{(A-7)}$$

$$\tau_{early,DT}(s_i) = \frac{9\pi^3}{16}\tau_{e,D}Z_{A,D}^4 s_i^4 \quad \text{(A-8)}$$

$$\tau_{late,DT}(s_i) = \sqrt{\frac{\pi^5}{6}}\tau_{e,D}Z_{A,D}^{3/2} \times \frac{\exp[U_{DT}(s_i)]}{\sqrt{s_i^2(1 - s_i)^{2\alpha} + \left(\frac{(1 + \alpha)}{3Z_{A,D}}\right)^{2\alpha/(1+\alpha)}\left(\Gamma\left[\frac{1}{(1 + \alpha)}\right]\right)^{-2}}} \quad \text{(A-9)}$$

To maintain the continuity of relaxation times after the constraint-release Rouse regime, the combined arm retraction time after τ_C is written in terms of τ_C[16]

$$\tau_A(s_i) = \tau_C\frac{\tau_{A,DT}(s_i)}{\tau_{A,DT}(s_{AR})} \quad \text{(A-10)}$$

The full expression for $G(\omega)$ with $G_e = (5/4)G_N$ and the terminal time τ_d in eq 6 is

$$\begin{aligned} G(\omega) = {} & G_e\phi_B\left(\frac{1}{5Z_B}\sum_{k=1}^{Z_B-1}\frac{i\omega\tau_e Z_B^2}{k^2 + i\omega\tau_e Z_B^2} + \frac{1}{Z_B}\sum_{k=Z_B}^{N_B}\frac{i\omega\tau_e Z_B^2}{2k^2 + i\omega\tau_e Z_B^2}\right) + \\ & G_e\phi_A\left(\frac{1}{5Z_A}\sum_{k=1}^{Z_A-1}\frac{i\omega\tau_e Z_A^2}{k^2 + i\omega\tau_e Z_A^2} + \frac{1}{Z_A}\sum_{k=Z_A}^{N_A}\frac{i\omega\tau_e Z_A^2}{2k^2 + i\omega\tau_e Z_A^2}\right) + \\ & G_N(1 + \alpha)\phi_B\int_0^1 (1 - g_B s_B)^\alpha\frac{i\omega\tau_{B,b}(s_B)}{1 + i\omega\tau_{B,b}(s_B)}\,ds_B + \\ & G_N(1 + \alpha)\phi_A\int_0^{s_{AR}}(1 - g_A s_A)^\alpha\frac{i\omega\tau_{A,b}(s_A)}{1 + i\omega\tau_{A,b}(s_A)}\,ds_A + \\ & G_N\phi_A(1 - s_{AR})\int_{\tau_{a,B}}^{\tau_C}\frac{\Phi(\tau)^\alpha}{2\tau}\frac{i\omega\tau}{1 + i\omega\tau}\,d\tau + \\ & G_N(1 + \alpha)\phi_A^{\alpha+1}\int_{s_{AR}}^{s_d}(1 - s)^\alpha\frac{i\omega\tau_A(s)}{1 + i\omega\tau_A(s)}\,ds + \\ & G_N(\phi_{Rbb}(1 - s_d))^{\alpha+1}\sum_{q=odd}\frac{8}{\pi^2 q^2}\frac{i\omega\tau_d}{q^2 + i\omega\tau_d} \end{aligned} \quad \text{(A-11)}$$

The first and second terms are the contributions of the free Rouse relaxation of each arm. The third and fourth terms correspond to the arm retraction process of each arm. The fifth term describes the constraint-release Rouse process after the relaxation of the short arm. The sixth term is the arm retraction process of the remaining long arms. The final term comes from the terminal reptation of the remaining backbone.

References and Notes

(1) Pearson, D. S.; Helfand, E. *Macromolecules* **1984**, *17*, 888.
(2) Milner, S. T.; McLeish, T. C. B. *Macromolecules* **1997**, *30*, 2159.
(3) McLeish, T. C. B.; et al. *Macromolecules* **1999**, *32*, 6738.
(4) Islam, M. T.; Juliani; Archer, L. A. Varshney, S. K. *Macromolecules* **2001**, *34*, 6438.
(5) Juliani; Archer L. A. *Macromolecules* **2002**, *35*, 10048.
(6) Archer, L. A.; Juliani. *Macromolecules* **2004**, *37*, 1076.
(7) Daniels, D. R.; McLeish, T. C. B.; Crosby, B. J.; Yong, R. N.; Fernyhough, C. M. *Macromolecules* **2001**, *34*, 7025.
(8) Gell, C. B.; Graessley, W. W.; Efstratiadis, V.; Pitsikalis, M.; Hadjichrstidis, N. *J. Polym. Sci., Part B: Polym. Phys.* **1997**, *35*, 1943.
(9) Frischknecht, A. L.; Milner, S. T.; Pryke, A.; Young, R. N.; Hawkins, R.; McLeish, T. C. B. *Macromolecules* **2002**, *35*, 4801.
(10) Tanaka, Y.; Takeuchi, Y.; Kobayashi, M.; Tadokoro, H. *J. Polym. Sci., Part A-2* **1971**, *9*, 43.
(11) Lee, J. H.; Fetters, L. J.; Archer, L. A.; Halasa, A. F. *Macromolecules*, in press.
(12) Gotro, J. T.; Graessley, W. W. *Macromolecules* **1984**, *17*, 2767.
(13) Abdel-Goad, M.; Pyckhout-Hintzen, W.; Kahle, S.; Allgaier, J.; Richter, D.; Fetter, L. J. *Macromolecules* **2004**, *37*, 8135.
(14) Frischknecht, A. L.; Milner, S. T. *Macromolecules* **2000**, *34*, 9764.
(15) Likhtman, A. E.; McLeish, T. C. B. *Macromolecules* **2002**, *35*, 6332.
(16) Milner, S. T.; McLeish, T. C. B.; Young R. N.; Hakiki, A.; Johnson, J. M. *Macromolecules* **1998**, *31*, 9345.
(17) Watanabe, H.; Matsumiya, Y.; Inoue, T. *Macromolecules* **2002**, *35*, 2339.
(18) Fetters, L. J.; Lohse, D.J.; Richter, D.; Witten, T. A.; Zirkel, A. *Macromolecules* **1994**, *27*, 4639.

MA047687I